Supporting Information

Stable lanthanide metal-organic frameworks as ratio fluorescent probe for efficient detection of riboflavin †

Xue-Chun Sun, [†] *Zhen-Zhong Cong,* [†] *Shuang-Yan Wu,* [†] *Ying Zhang*[*,†] *Ming-Chang Zhu*[*,†] *and Xiao-Jue Bai*[*,‡]

[†]The Key Laboratory of the Inorganic Molecule-Based Chemistry of Liaoning Province and Laboratory of Coordination Chemistry, Shenyang University of Chemical Technology, Shenyang 110142, P. R. China.

E-mail: zhangy621@syuct.edu.cn, mczhu@syuct.edu.cn

[‡]Chinese Academy of Sciences (CAS) Key Laboratory of Nanosystem and Hierarchy Fabrication, National Center for Nanoscience and Technology, Beijing 100190, P. R. China.

E-mail: baixj2021@nanoctr.cn

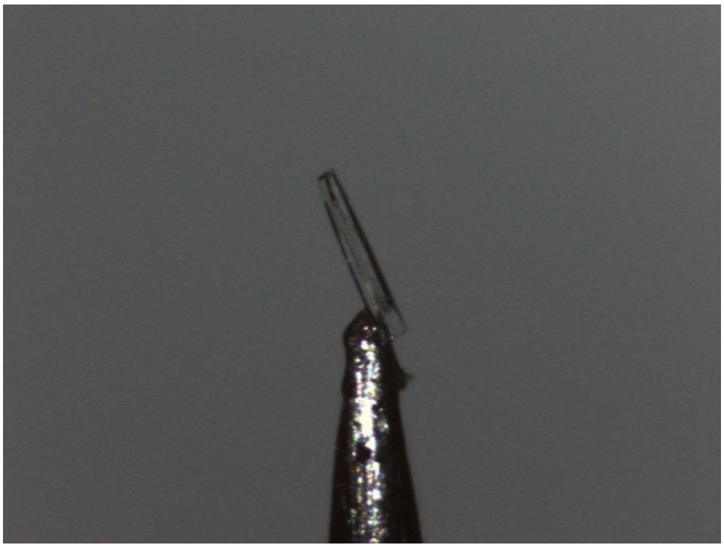
Fig. S1 Single crystal picture of Eu-BPTA.

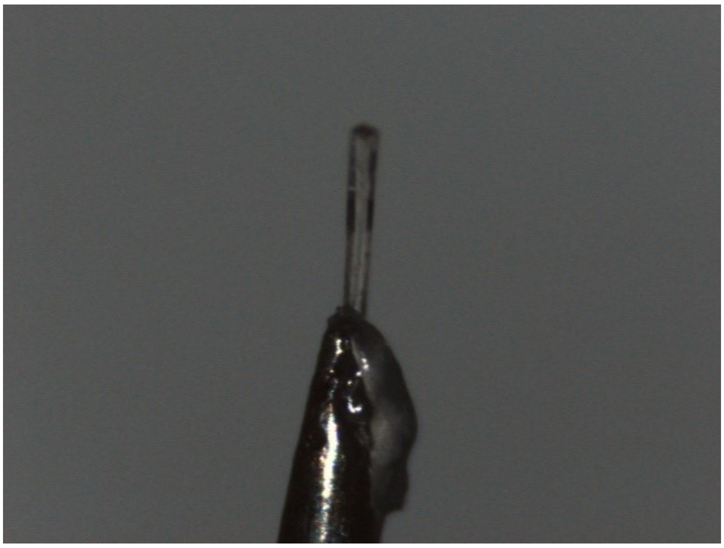

Fig. S2 Single crystal picture of Sm-BPTA.

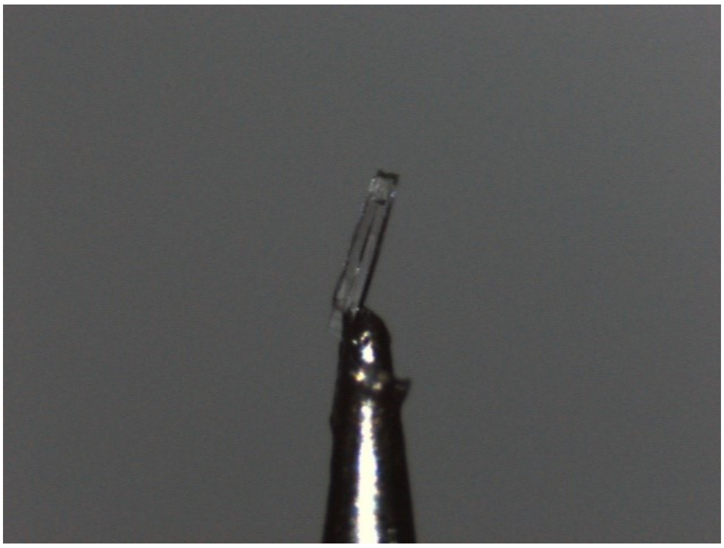

Fig. S3 Single crystal picture of Sm-BPTA.

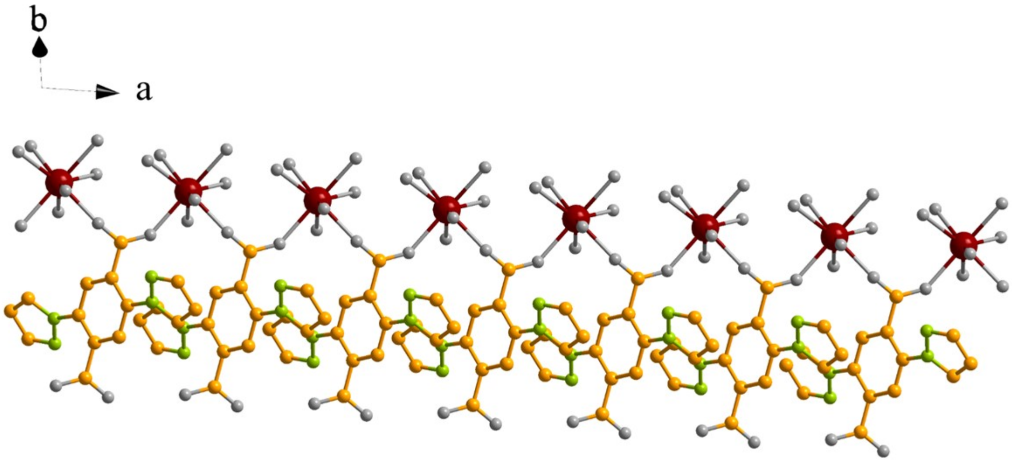

Fig. S4 One dimensional chain of Ln-BPTA.

Table S1 Crystal data and structure refinement for Eu-BPTA

Empirical formula	**$C_{21}H_{18}N_6O_9Eu$**
Formula weight	650.37
Temperature/K	293.15
Crystal system	triclinic
Space group	P-1
a/Å	5.2645(2)
b/Å	13.1605(7)
c/Å	16.6532(9)
α/°	97.157(4)
β/°	96.532(4)
γ/°	92.653(4)
Volume/$Å^3$	1135.23(10)
Z	2
ρ_{calc} g/cm^3	1.903
μ/mm-1	2.830
F (000)	642.0
Crystal size/mm^3	0.1 × 0.1 × 0.1
Radiation	Mo Kα (λ = 0.71073)
2Θ range for data collection/°	5.512 to 65.06
Index ranges	$-7 \leq h \leq 7$, $-19 \leq k \leq 19$, $-24 \leq l \leq 25$
Reflections collected	19462
Data/restraints/parameters	7686/0/358
Final R indexes [I>=2σ (I)]	R_1 = 0.0338, wR_2 = 0.0662
Final R indexes [all data]	R_1 = 0.0476, wR_2 = 0.0712
Largest diff. peak/hole / e $Å^{-3}$	2.62/-0.91
CCDC	2128999

Table S2 Bond Lengths for Eu-BPTA

Bond	**Length/Å**	**Bond**	**Length/Å**
Eu1-O6	2.448 (2)	Eu1-O73	2.385 (2)
Eu1-O8	2.518 (2)	Eu1-O89	2.450 (2)
Eu1-O9	2.494 (2)	Eu1-O133	2.3713 (18)
Eu1-O52	2.3295 (19)	Eu1-O168	2.298 (2)

[1]1+X, +Y, +Z; [2]1-X, 1-Y, 1-Z; 3-X, -Y, -Z; [4]2-X, 1-Y, -Z

Table S3 Bond Angles for Eu-BPTA

Bond	**Angle/°**	**Bond**	**Angle/°**
O6-Eu1-O8	73.21 (7)	O89-Eu1-O8	143.81 (8)
O6-Eu1-O9	72.23 (7)	O89-Eu1-O9	137.00 (8)
O6-Eu1-O89	139.75 (9)	O133-Eu1-O6	92.01 (7)
O9-Eu1-O8	51.77 (6)	O133-Eu1-O8	124.59 (7)
O52-Eu1-O6	100.25 (7)	O133-Eu1-O9	72.82 (7)
O52-Eu1-O8	72.14 (7)	O133-Eu1-O73	87.44 (7)
O52-Eu1-O9	123.49 (7)	O133-Eu1-O89	77.46 (8)
O52-Eu1-O73	84.08 (7)	O168-Eu1-O6	147.63 (8)
O52-Eu1-O89	84.65 (8)	O168-Eu1-O8	78.36 (8)
O52-Eu1-O133	161.95 (8)	O168-Eu1-O9	78.18 (7)
O73-Eu1-O6	71.20 (7)	O168-Eu1-O52	85.18 (7)
O73-Eu1-O8	132.32 (7)	O168-Eu1-O73	141.11 (8)
O73-Eu1-O9	137.45 (7)	O168Eu1-O89	72.23 (9)
O73-Eu1-O89	69.62 (9)	O168-Eu1-O133	91.55 (7)

^{1}1+X, +Y, +Z; ^{2}1-X, 1-Y, 1-Z; ^{3}-X, -Y, -Z; ^{4}-1+X, +Y, +Z; ^{5}2-X, 1-Y, -Z

Table S4 Crystal data and structure refinement for Sm-BPTA

Empirical formula	$\mathbf{C_{21}H_{18}N_6O_9Sm}$
Formula weight	648.76
Temperature/K	298.0
Crystal system	triclinic
Space group	P-1
a/Å	5.2631(3)
b/Å	13.1534(7)
c/Å	16.6741(10)
α/°	97.062(5)
β/°	96.554(5)
γ/°	92.507(5)
Volume/$Å^3$	1136.11(11)
Z	2
ρ_{calc} g/cm^3	1.896
μ/mm^{-1}	2.652
F (000)	640.0
Crystal size/mm^3	0.1 × 0.1 × 0.1
Radiation	Mo Kα (λ = 0.71073)
2Θ range for data collection/°	5.512 to 50.056
Index ranges	$-6 \le h \le 6$, $-15 \le k \le 15$, $-19 \le l \le 19$
Reflections collected	12484
Data/restraints/parameters	4022/0/346
Goodness-of-fit on F^2	1.132
Final R indexes [I>=2σ (I)]	R_1 = 0.0252, wR_2 = 0.0625
Final R indexes [all data]	R_1 = 0.0288, wR_2 = 0.0647
Largest diff. peak/hole / e Å^{-3}	1.39/-0.50
CCDC	2184517

Table S5 Bond Lengths for Sm-BPTA

Bond	**Length/Å**	**Bond**	**Length/Å**
Sm1-O1	2.392(3)	Sm1-O11	2.525(3)
Sm1-O2	2.505(3)	Sm1-O15	2.458(3)
Sm1-O4[1]	2.383(2)	Sm1-O16	2.460(4)
Sm1-O7	2.342(3)	Sm1-O17	2.308(3)

[1]1+X, +Y, +Z; [2]-1-X, 1-Y, -Z; 3-X, 2-Y, 1-Z; [4]1-X, 2-Y, -Z

Table S6 Bond Angles for Sm-BPTA

Bond	**Angle/°**	**Bond**	**Angle/°**
O1-Sm1-O2	137.35(9)	O7-Sm1-O15	100.46(11)
O1-Sm1-O11	132.58(10)	O7-Sm1-O16	84.86(12)
O1-Sm1-O15	71.46(10)	O15-Sm1-O2	71.95(10)
O1-Sm1-O16	69.27(12)	O15-Sm1-O11	73.01(10)
O2-Sm-O11	51.55(9)	O15-Sm1-O16	139.64(12)
$O4^{1}$-Sm1-O1	87.14(9)	O16-Sm1-O2	137.16(12)
$O4^{1}$ -Sm1-O2	72.74(9)	O16-Sm1-O11	144.23(11)
$O4^{1}$-Sm1-O11	124.29(9)	O17-Sm1-O1	140.98(10)
$O4^{1}$ -Sm1-O15	91.61(10)	O17-Sm1-O2	78.33(10)
$O4^{1}$ -Sm1-O16	77.58(11)	O17-Sm1-$O4^{1}$	91.90(9)
O7-Sm1-O1	84.53(9)	O17-Sm1-O7	84.87(10)
O7-Sm1-O2	123.25(9)	O17-Sm1-O11	78.40(10)
O7-Sm1-$O4^{1}$	162.30(10)	O17-Sm1-O15	147.51(10)
O7-Sm1-O11	72.14(9)	O17-Sm1-O16	72.45(12)

^{1}1+X, +Y, +Z; ^{2}-1+X, +Y, +Z; ^{3}-1-X, 1-Y, -Z; ^{4}-X, 2-Y, 1-Z; ^{5}1-X, 2-Y, -Z

Table S7 Crystal data and structure refinement for Dy-BPTA

Empirical formula	**$C_{21}H_{18}N_6O_9Dy$**
Formula weight	660.91
Temperature/K	298
Crystal system	triclinic
Space group	P-1
a/Å	5.2345(3)
b/Å	13.1182(12)
c/Å	16.6342(12)
α/°	97.377(7)
β/°	96.786(5)
γ/°	92.674(6)
Volume/Å^3	1122.61(14)
Z	2
ρ_{calc} g/cm^3	1.952
μ/mm^{-1}	3.396
F (000)	646.0
Crystal size/mm^3	0.3 × 0.1 × 0.1
Radiation	Mo Kα (λ = 0.71073)
2Θ range for data collection/°	5.514 to 56.558
Index ranges	$-6 \le h \le 6$, $-17 \le k \le 17$, $-22 \le l \le 22$
Reflections collected	5550
Data/restraints/parameters	5550/0/347
Goodness-of-fit on F^2	1.160
Final R indexes [I>=2σ (I)]	R_1 = 0.0799, wR_2 = 0.2081
Final R indexes [all data]	R_1 = 0.0880, wR_2 = 0.2129
Largest diff. peak/hole / e Å^{-3}	6.18/-4.89
CCDC	2184518

Table S8 Bond Lengths for Dy-BPTA

Bond	**Length/Å**	**Bond**	**Length/Å**
Dy1-O4	2.334(9)	Dy1-O16	2.397(10)
Dy1-O5[1]	2.302(9)	Dy1-O18	2.246(9)
Dy1-O8	2.410(10)	Dy1-O19[1]	2.346(9)
Dy- O14	2.494(9)	Dy1-O26	2.472(9)

[1]-1+X, +Y, +Z; [2]2-X, 2-Y, 1-Z; [3]1-X, 2-Y, -Z; [4]1-X, 1-Y, -Z

Table S9 Bond Angles for Dy-BPTA

Bond	**Angle/°**	**Bond**	**Angle/°**
O4-Dy1-O8	77.7(4)	O16-Dy1-O14	73.0(4)
O4-Dy1-O14	125.6(3)	O16-Dy1-O26	72.4(4)
O4-Dy1-O16	91.9(4)	O18-Dy1-O4	92.2(3)
O4-Dy1-O19^{1}	87.0(3)	O18-Dy1-O5^{1}	84.7(3)
O4-Dy1-O26	73.1(3)	O18-Dy1-O8	72.9(4)
O5^{1-}Dy1-O4	161.2(3)	O18-Dy1-O14	78.4(4)
O5^{1}Dy1-O8	83.7(4)	O18-Dy1-O16	147.4(4)
O5^{1}-Dy1-O14	72.0(3)	O18-Dy1-O19^{1}	141.6(4)
O5^{1}-Dy1-O16	100.7(4)	O18-Dy1-O26	77.9(3)
O5^{1}-Dy1-O19^{1}	84.0(3)	O19^{1}-Dy1-O8	69.4(4)
O5^{1}-Dy1-O26	123.9(3)	O19^{1}-Dy1-O14	131.6(4)
O8-Dy1-O14	143.8(3)	O19^{1}-Dy1-O16	71.0(4)
O8-Dy1-O26	137.4(3)	O19^{1}-Dy1-O26	137.4(3)
O16-Dy1-O8	139.5(4)	O26-Dy1-O14	52.5(3)

^{1}-1+X, +Y, +Z; ^{2}1+X, +Y, +Z; ^{3}2-X, 2-Y, 1-Z; ^{4}1-X, 2-Y, -Z; ^{5}1-X, 1-Y, -Z

Table S10 Crystal data and structure refinement for Tb-BPTA

Empirical formula	**$C_{21}H_{18}N_6O_9Tb$**
Formula weight	657.33
Temperature/K	293
Crystal system	triclinic
Space group	P-1
a/Å	5.2418(3)
b/Å	13.1733(9)
c/Å	16.6632(13)
α/°	97.418(6)
β/°	96.798(5)
γ/°	92.733(5)
Volume/Å3	1130.65(14)
Z	2
ρcalcg/cm3	1.931
μ/mm-1	3.195
F (000)	646.0
Crystal size/mm3	0.1 × 0.1 × 0.1
Radiation	Mo Kα (λ = 0.71073)
2θ range for data collection/°	5.5 to 50.052
Index ranges	$-6 \leq h \leq 6$, $-15 \leq k \leq 15$, $-19 \leq l \leq 19$
Reflections collected	3997
Data/restraints/parameters	3997/0/343
Final R indexes [I>=2σ (I)]	R1 = 0.0335, wR2 = 0.0692
Final R indexes [all data]	R1 = 0.0400, wR2 = 0.0732
Largest diff. peak/hole / e Å-3	1.57/-1.67
CCDC	2128987

Table S11 Bond Lengths for Tb-BPTA

Bond	**Length/Å**	**Bond**	**Length/Å**
Tb1-O1	2.339(4)	Tb1-O23	2.425(5)
Tb1-O3	2.306(4)	Tb1-O25	2.507(4)
Tb1-O5[1]	2.375(4)	Tb1-O31	2.423(4)
Tb1-O6	2.483(3)	Tb1-O9	2.271(4)

[1]-1+X, +Y, +Z; [2]1+X, +Y, +Z; [3]-1-X, 1-Y, -Z; [4]2-X, 2-Y, 1-Z; [5]1-X, 2-Y, -Z

Table S12 Bond Angles for Tb-BPTA

Bond	**Angle/°**	**Bond**	**Angle/°**
O1-Tb1-O5^1	87.18(13)	O6-Tb1-O25	52.01(12)
O1-Tb1-O6	72.89(13)	O9-Tb1-O1	91.74(13)
O1-Tb1-O23	77.63(15)	O9-Tb1-O3	85.19(14)
O1-Tb1-O25	124.89(13)	O9-Tb1-O5^1	141.42(14)
O1-Tb1-O31	91.90(13)	O9-Tb1-O6	78.02(13)
O3-Tb1-O1	161.59(13)	O9-Tb1-O23	72.87(17)
O3-Tb1-O5^1	84.03(13)	O9-Tb1-O25	78.34(14)
O3-Tb1-O6	123.83(13)	O9-Tb1-O31	147.33(14)
O3-Tb1-O23	84.13(16)	O23-Tb1-O6	137.45(16)
O3-Tb1-O25	72.27(13)	O23-Tb1-O25	144.04(15)
O3-Tb1-O31	100.47(14)	O31-Tb1-O6	72.12(13)
O5^1-Tb1-O6	137.27(13)	O31-Tb1-O23	139.44(16)
O5^1 -Tb1-O23	69.24(16)	O31-Tb1-O25	73.03(14)
O5^1-Tb1-O25	132.09(14)	O5^1 -Tb1-O31	71.20(13)

^{1}-1+X, +Y, +Z; ^{2}1+X, +Y, +Z; ^{3}-1-X,1-Y, -Z; ^{4}2-X, 2-Y, 1-Z; ^{5}1-X, 2-Y, -Z

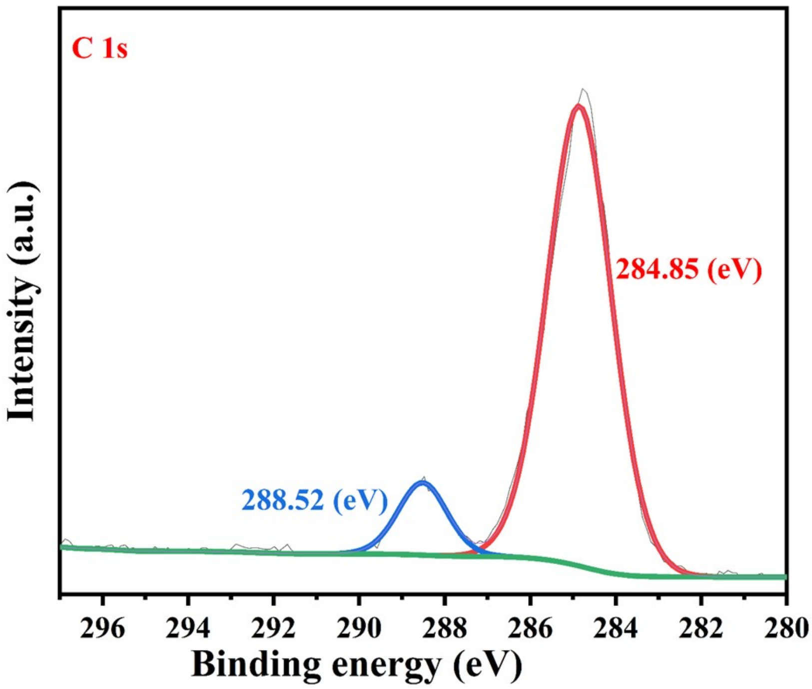

Fig. S5 XPS high-resolution spectra of C 1s.

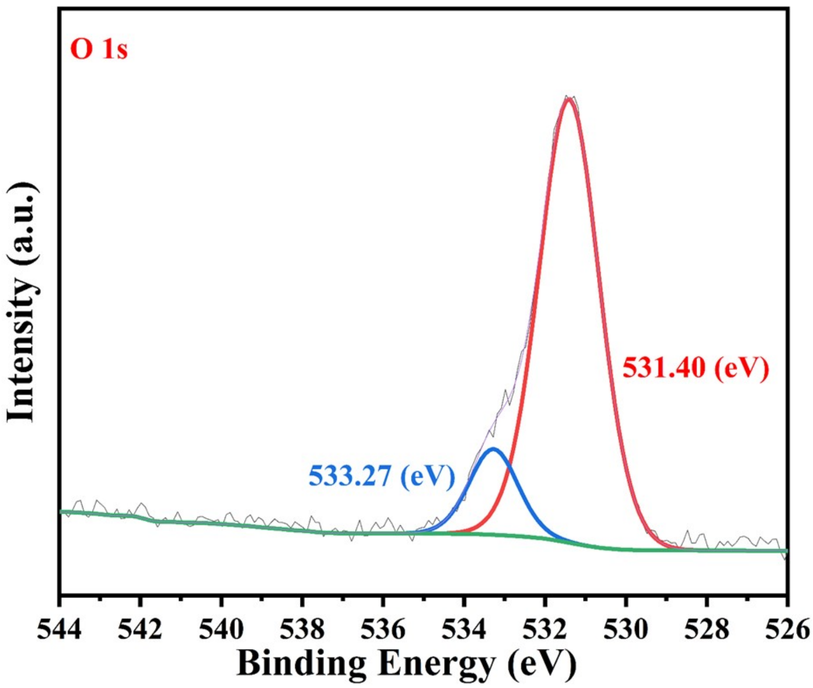

Fig. S6 XPS high-resolution spectra of O 1s.

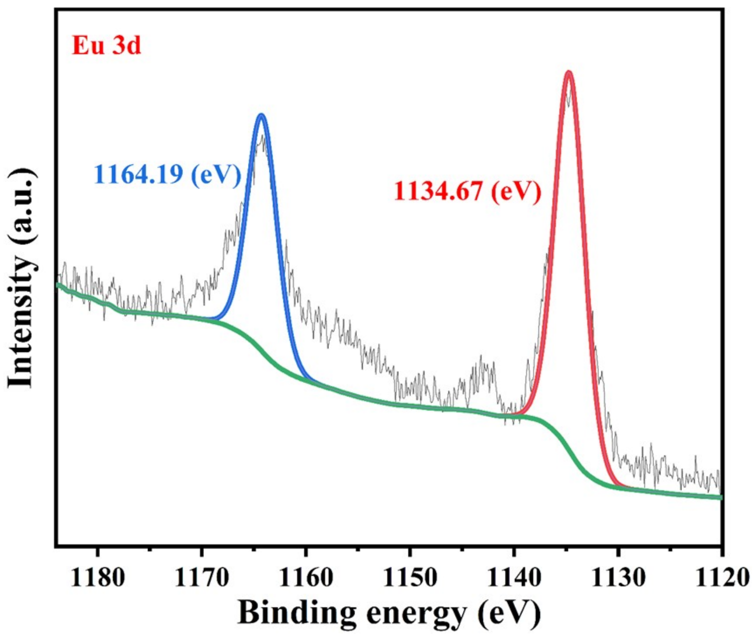

Fig. S7 XPS high-resolution spectrum of Eu 3d.

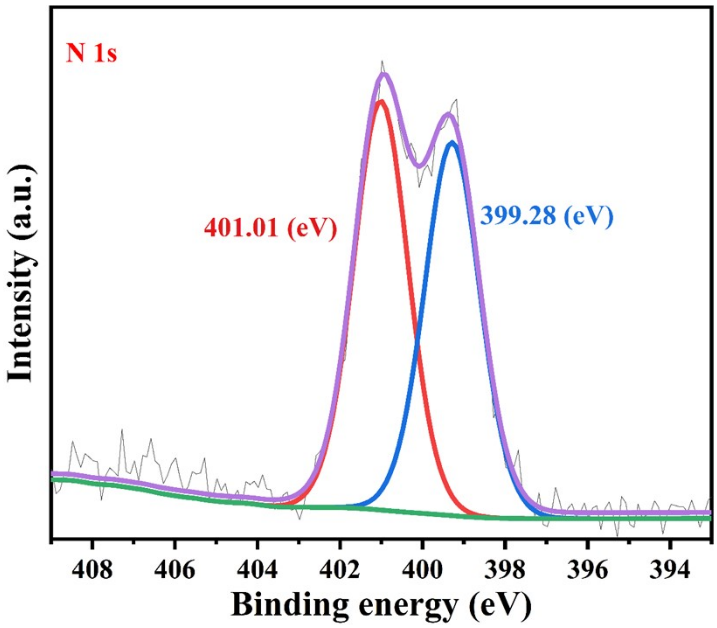

Fig. S8 XPS high-resolution spectrum of N 1s

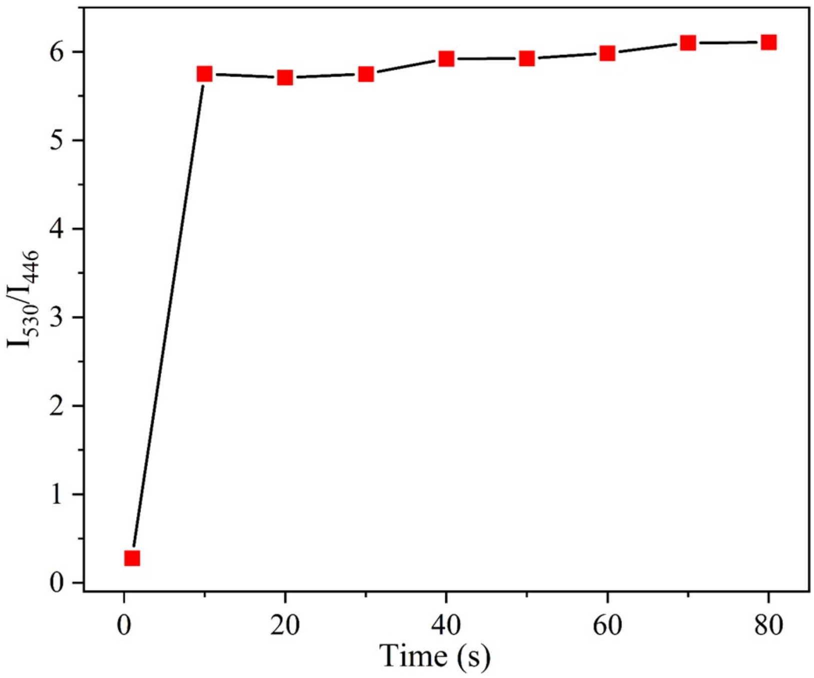

Fig. S9 Response time curve of Eu-BPTA

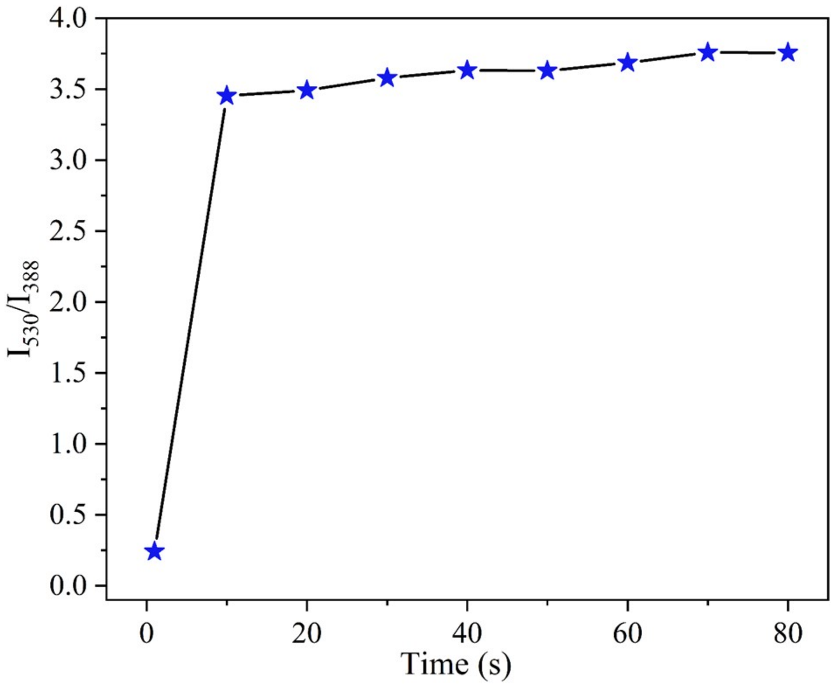

Fig. S10 Response time curve of Sm-BPTA

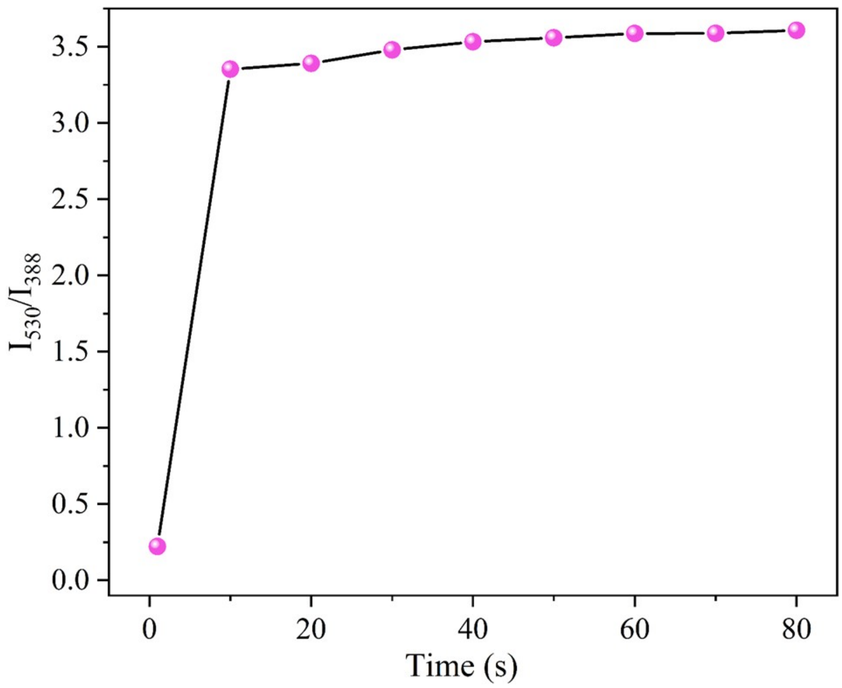

Fig. S11 Response time curve of Dy-BPTA

Table S13 Limit of detection of different detector for RF

Material	Matrices	LOD (nM)	Ref
g-C3N4	Milk and drink	170	S1
g-CNQDs@Zn-MOF	Milk	15	S2
NPCDs	Milk and riboflavin pharmaceutical tablets	170	S3
N, S-CDs	DI water	1.9	S4
AHNPs	Pharmaceutical samples	71	S5
g-CNQDs	Vitamin B2 and human serum	0.63	S6
Ag@SiO2	Water	100	S7
HPLC-SFS	Drink	5.3	S8
NPCl-CQDs	River Water and human urine	3.59	S9
sulfonated graphene (SG)	DNA, RNA, lysine, BSA, blood serum	1.6	S10
Eu-BPTA $\{[Eu(C_{14}H8N_4O_4)_{1.5}\cdot 2H_2O]\cdot H_2O\}_n$	Milk, fetal bovine serum and energy drinks	5.02	This work
Sm-BPTA $\{[Sm(C_{14}H8N_4O_4)_{1.5}\cdot 2H_2O]\cdot H_2O\}_n$	Milk, fetal bovine serum and energy drinks	8.56	This work
Dy-BPTA $\{[Dy(C_{14}H8N_4O_4)_{1.5}\cdot 2H_2O]\cdot H_2O\}_n$	Milk, fetal bovine serum and energy drinks	8.62	This work

[S1] J. Han, H. Y. Zou, M. X. Gao and C. Z. Huang, *Talanta*, 2016, **148**, 279-284.

[S2] S. Feng, F. Pei, Y. Wu, J. Lv, Q. Hao, T. Yang, Z. Tong and W. Lei, *Spectrochim. Acta. A Mol. Biomol.Spectrosc.*, 2021, **246**, 119004.

]S3] L. Lin, Y. Wang, Y. Xiao and X. Chen, *Anal. Bioanal. Chem.*, 2019, **411**, 2803-2808.

[S4] J. Wang, S. Su, J. Wei, R. Bahgi, L. Hope-Weeks, J. Qiu and S. Wang, *Physica E*, 2015, **72**, 17-24.

[S5] P. G. Mahajan, N. C. Dige, S. B. Suryawanshi, D. K. Dalavi, A. A. Kamble, D. P. Bhopate, A. N. Kadam, V. V. Kondalkar, G. B. Kolekar and S. R. Patil, *JFlu*, 2018, **28**, 207-215.

[S6] H. Wang, Q. Ma, Y. Wang, C. Wang, D. Qin, D. Shan, J. Chen and X. Lu, *Anal. Chim. Acta*, 2017, **973**, 34-42.

[S7] J. Zhang, X. Li, J.-C. Zhang, J.-S. Yan, H. Zhu, J.-J. Liu, R. Li, S. Ramakrishna and Y.-Z. Long, *Chem. Eng. J.*, 2020, **382**, 122779.

[S8] L. Ziak, P. Majek, K. Hrobonova, F. Cacho and J. Sadecka, *Food Chem.*, 2014, **159**, 282-286.

[S9] Z. Wang, L. Zhang, Y. Hao, W. Dong, Y. Liu, S. Song, S. Shuang, C. Dong and X. Gong, *Anal. Chim. Acta*, 2021, **1144**, 1-13.

[S10] A. Kundu, S. Nandi, R. K. Layek and A. K. Nandi, *ACS Appl. Mater. Interfaces*, 2013, **5**, 7392-7399.

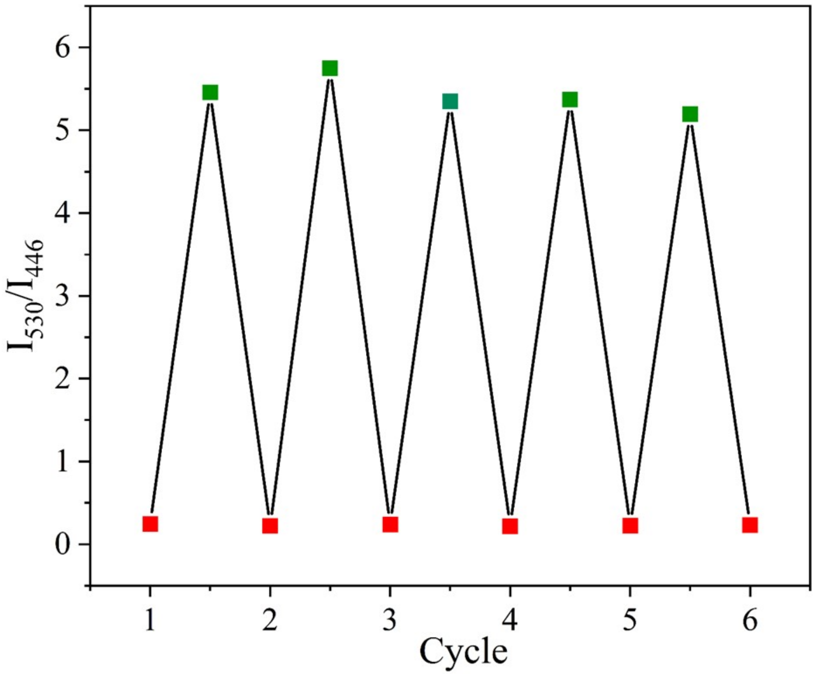

Fig. S12 The emission intensity ratio (I_{530}/I_{446}) of Eu-BPTA during the successive RF detection.

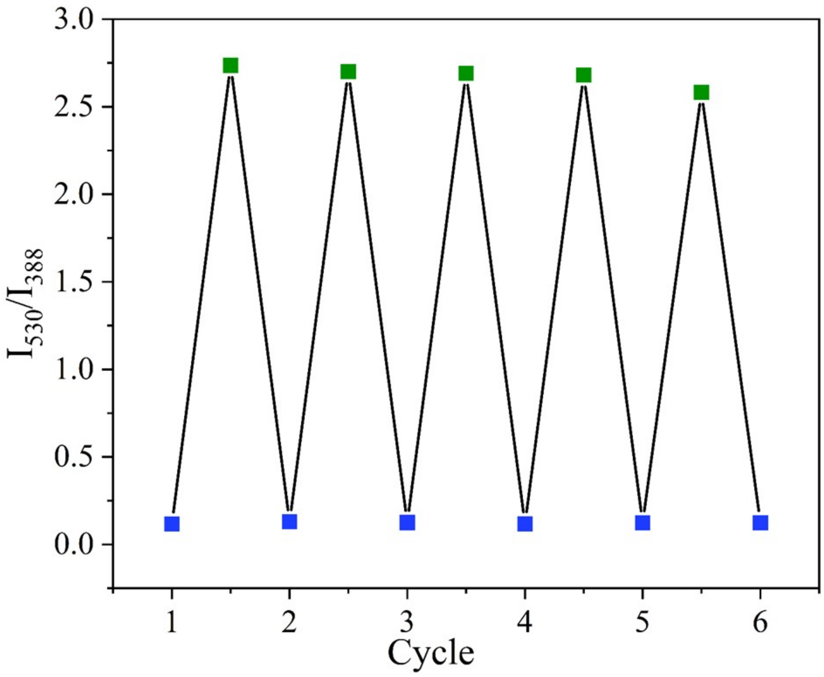

Fig. S13 The emission intensity ratio (I_{530}/I_{388}) of Sm-BPTA during the successive RF detection.

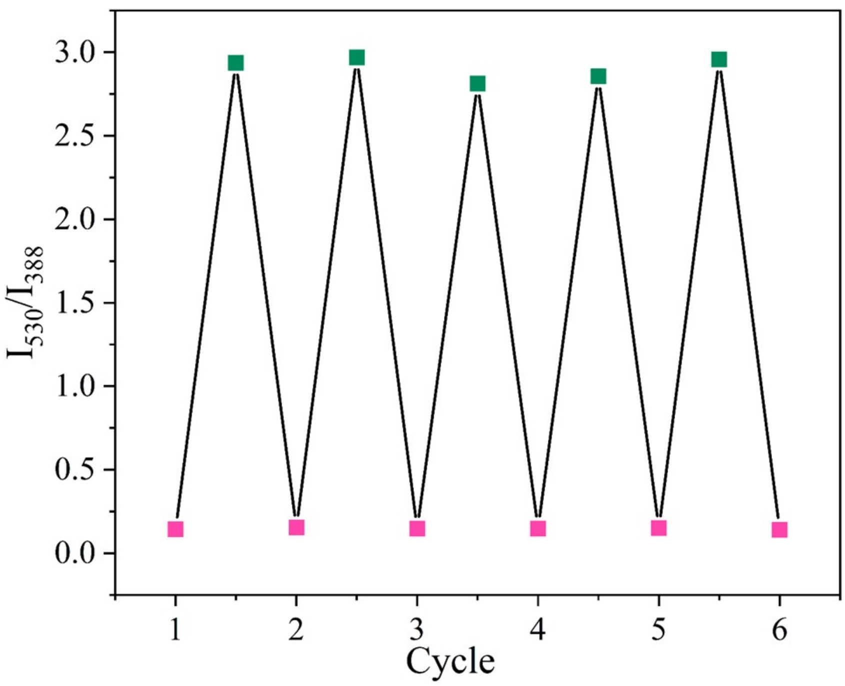

Fig. S14 The emission intensity ratio ($I_{530/388}$) of Dy-BPTA during the successive RF detection.

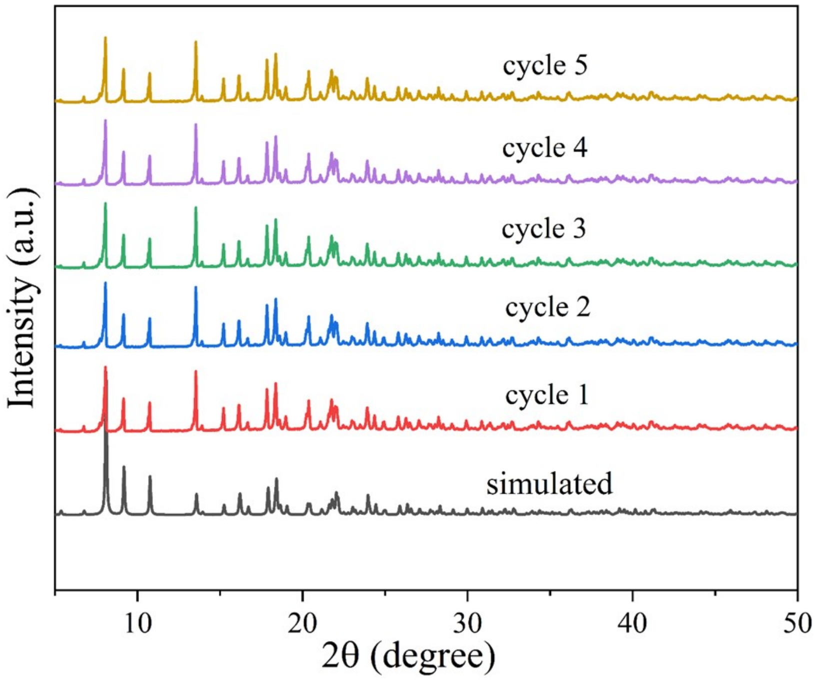

Fig. S15 PXRD patterns of Eu-BPTA after 5 cycles.

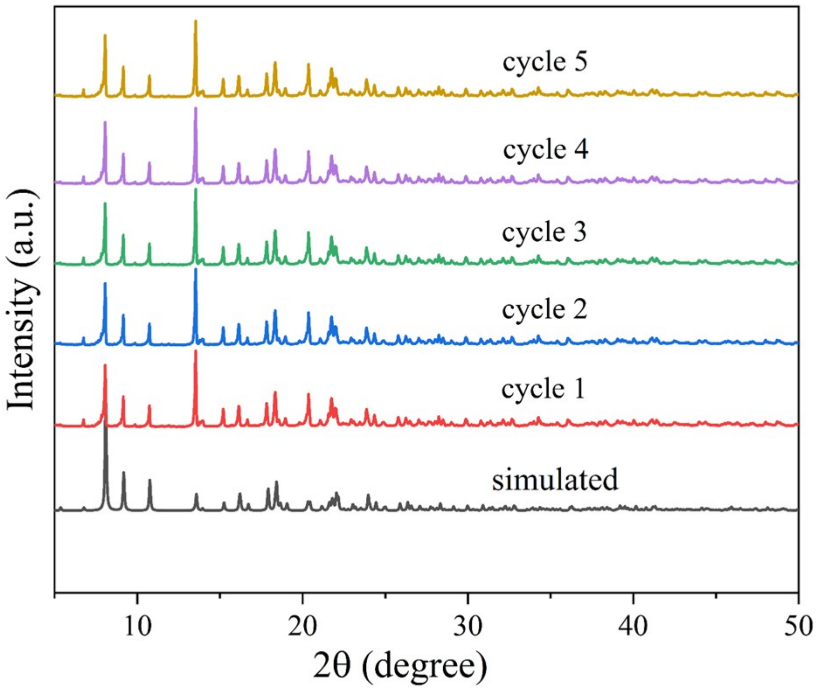

Fig. S16 PXRD patterns of Sm-BPTA after 5 cycles.

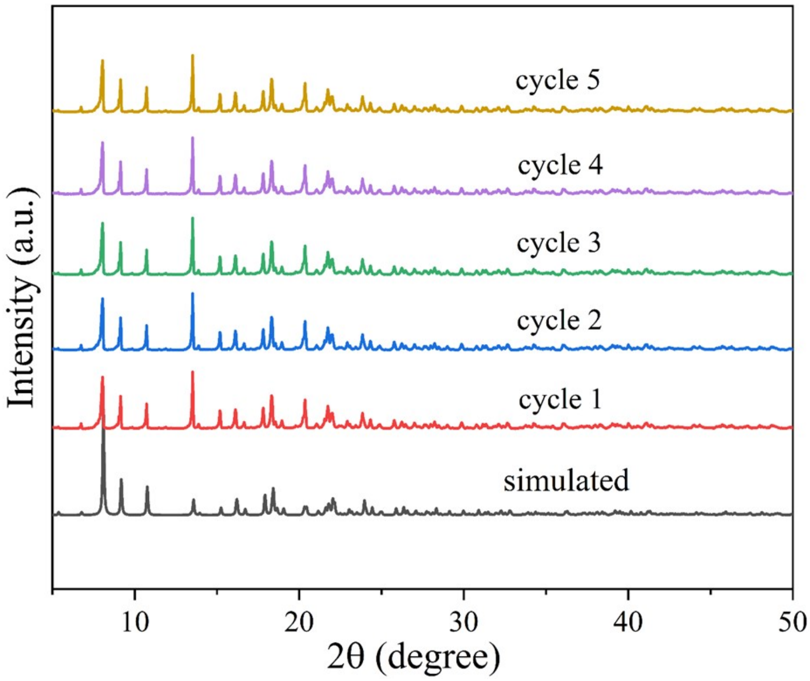

Fig. S17 PXRD patterns of Dy-BPTA after 5 cycles.

Table S14 Determination of RF in fetal bovine serum

Sample	Added value (μM)	Test value (μM)	Recovery (%)	RSD (%, n=3)
Eu-BPTA	4	3.6	90 %	1.2
	6	5.68	94.7 %	2.1
	10	9.84	98.4%	2.7
Sm-BPTA	4	3.7	92.5 %	2.5
	6	5.64	94 %	1.5
	10	9.54	95.4 %	2.8
Dy-BPTA	4	3.66	91.6%	3.2
	6	5.52	92%	4.6
	10	9.24	92.4%	5.3

Table S15 Determination of RF in milk

Sample	Added value (μM)	Test value (μM)	Recovery (%)	RSD (%, n=3)
Eu-BPTA	4	3.83	95.72 %	2.2
	6	5.97	99.57 %	4.1
	10	1.01	100.08%	1.4
Sm-BPTA	4	4.16	104.2 %	2.1
	6	5.98	99.98 %	3.5
	10	9.71	97.13 %	0.9
Dy-BPTA	4	4.2	105 %	5.4
	6	6.12	102 %	2
	10	10.7	107 %	2.6

Table S16 Determination of RF in energy drinks

Sample	Added value (μM)	Test value (μM)	Recovery (%)	RSD (%, n=3)
Eu-BPTA	4	3.86	96.61 %	2.2
	6	6.03	100.5 %	2.8
	10	10.05	104.6%	1.2
Sm-BPTA	4	3.76	94.08 %	2.7
	6	5.76	95.52 %	1.8
	10	10.5	105.07 %	6.0
Dy-BPTA	4	3.6	90 %	9.2
	6	5.72	95.38 %	5.5
	10	9.9	99 %	7.2

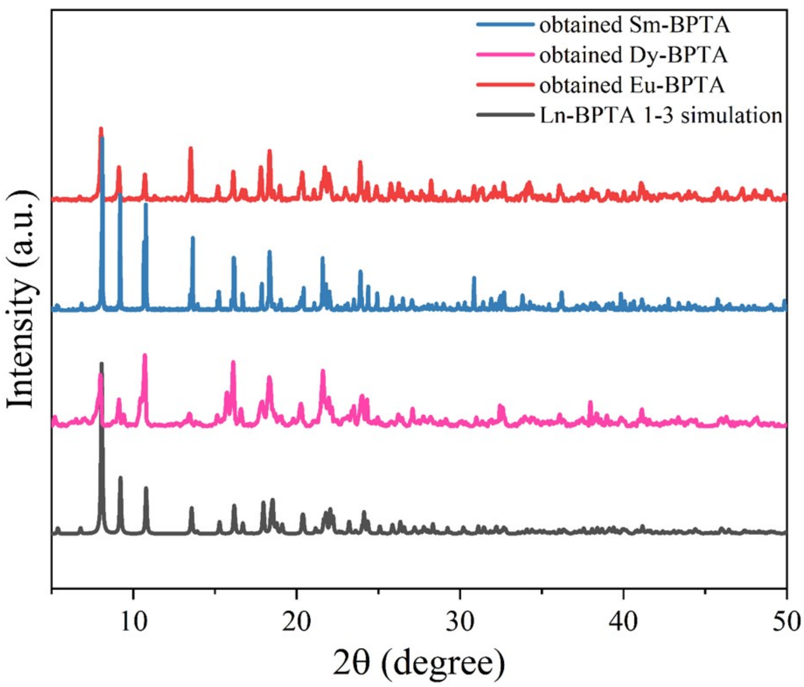

Fig. S18. PXRD pattern of Ln-BPTA 1-3 after immersion in water for 24 h

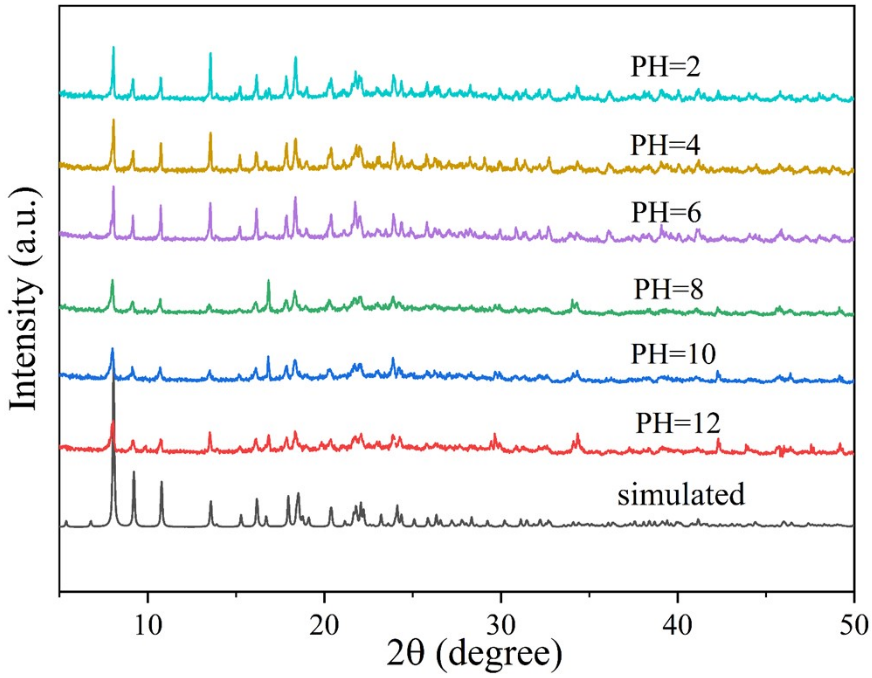

Fig. S19. PXRD diagram of Eu-BPTA immersed in solutions with different pH values (2 to 12).

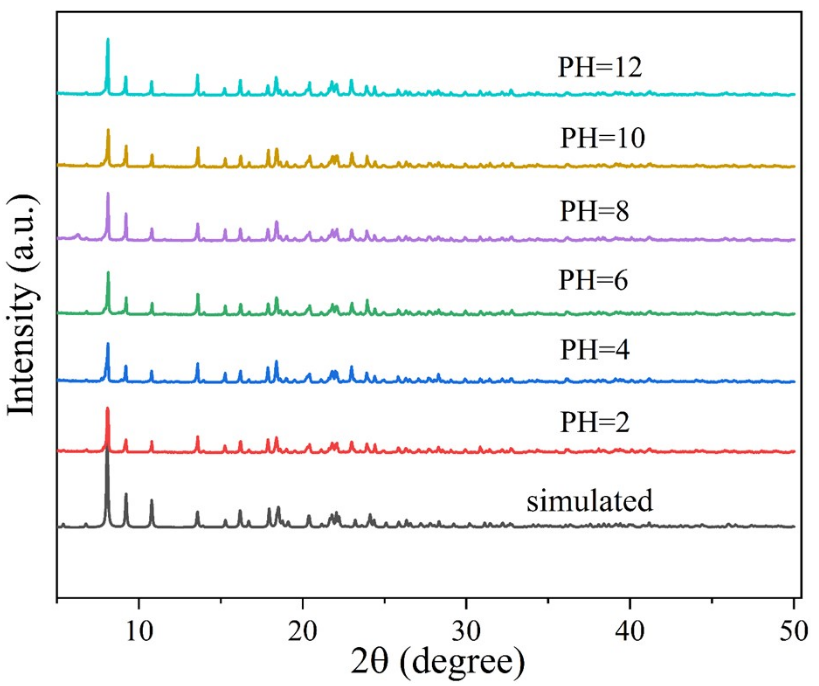

Fig. S20. PXRD diagram of Sm-BPTA immersed in solutions with different pH values (2 to 12).

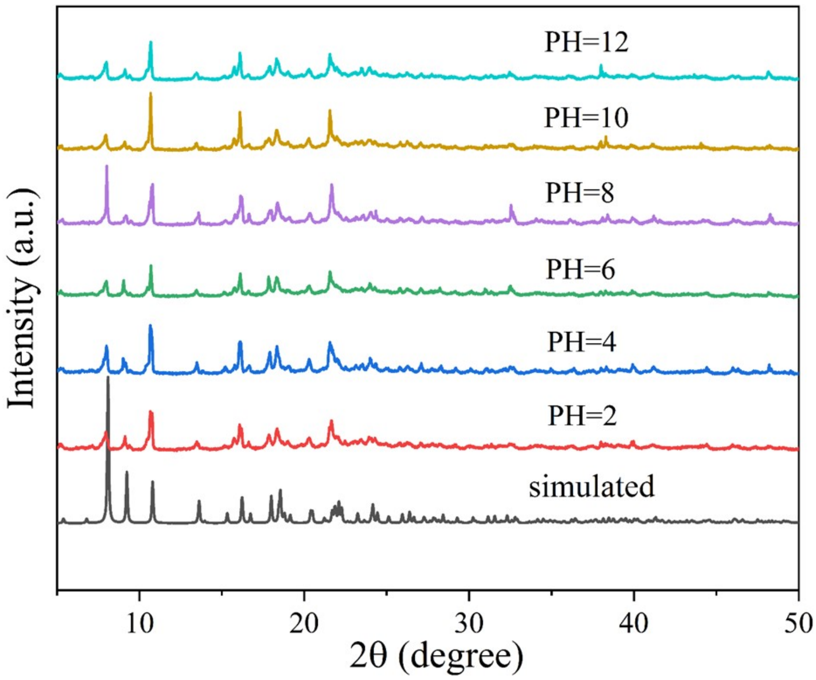

Fig. S21. PXRD diagram of Dy-BPTA immersed in solutions with different pH values (2 to 12).

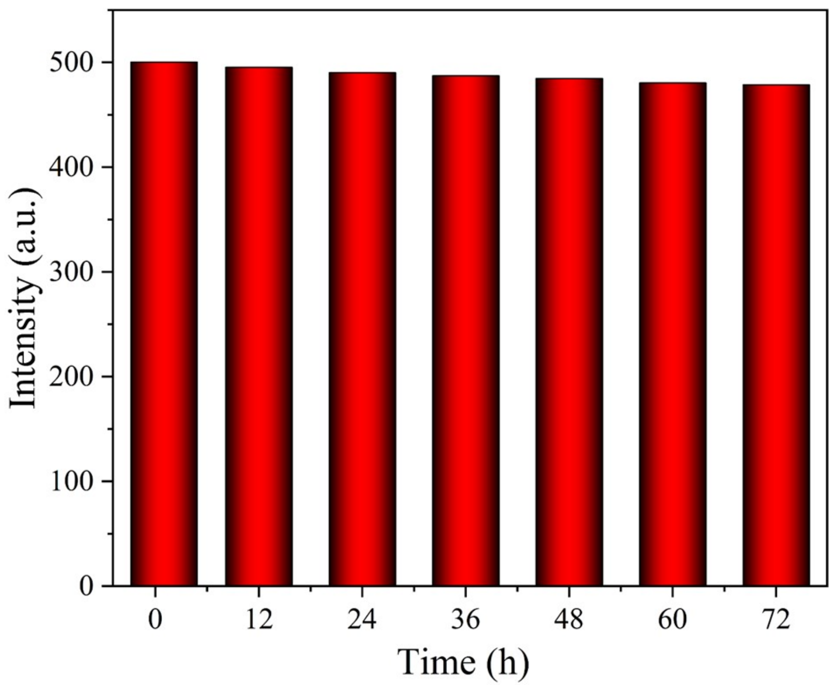

Fig. 22. Fluorescence intensity diagram of Eu-BPTA in water within three days

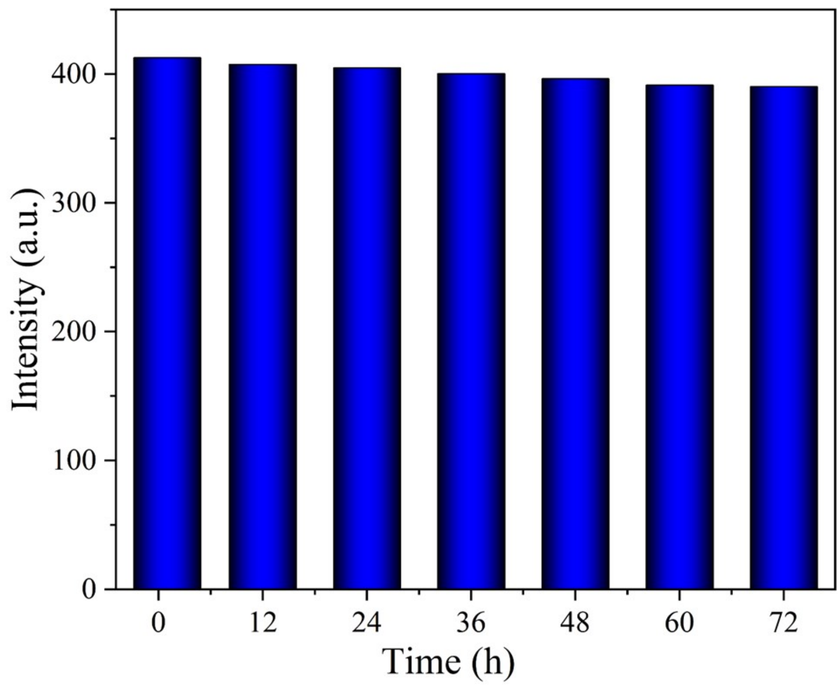

Fig. 23. Fluorescence intensity diagram of Sm-BPTA in water within three days

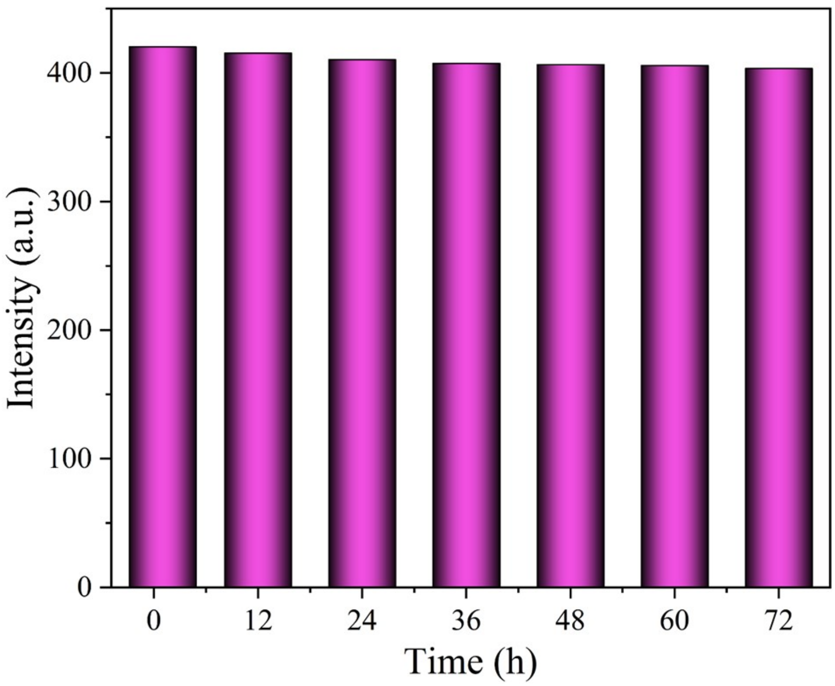

Fig. 24. Fluorescence intensity diagram of Dy-BPTA in water within three days

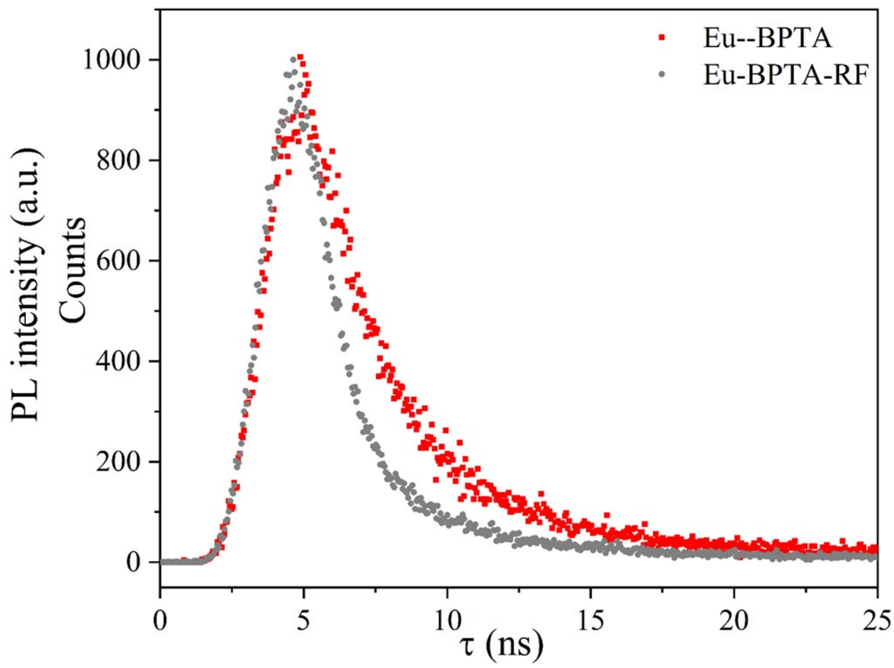

Fig. 25. Fluorescence lifetime change spectrum of Eu-BPTA after RF detection

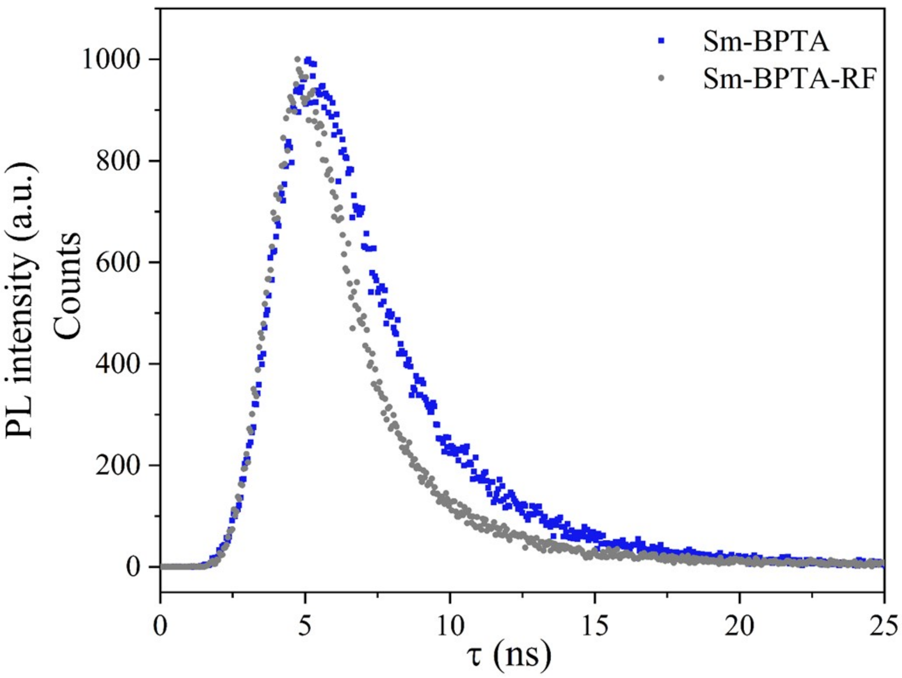

Fig. 26. Fluorescence lifetime change spectrum of Sm-BPTA after RF detection

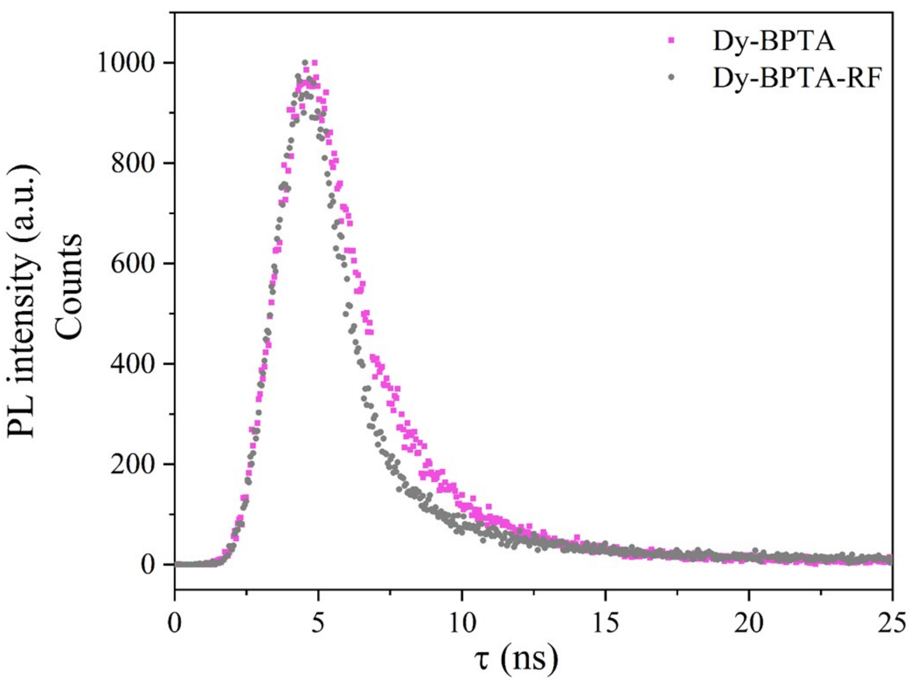

Fig. 27. Fluorescence lifetime change spectrum of Dy-BPTA after RF detection

Table S17. Change of fluorescence lifetime before and after Ln-BPTA detection

	Fluorescence lifetime (Ln-BPTA)	Fluorescence lifetime (Ln-BPTA-RF)
Eu-BPTA	3.69	2.33
Sm-BPTA	3.42	2.48
Dy-BPTA	3.67	3.21

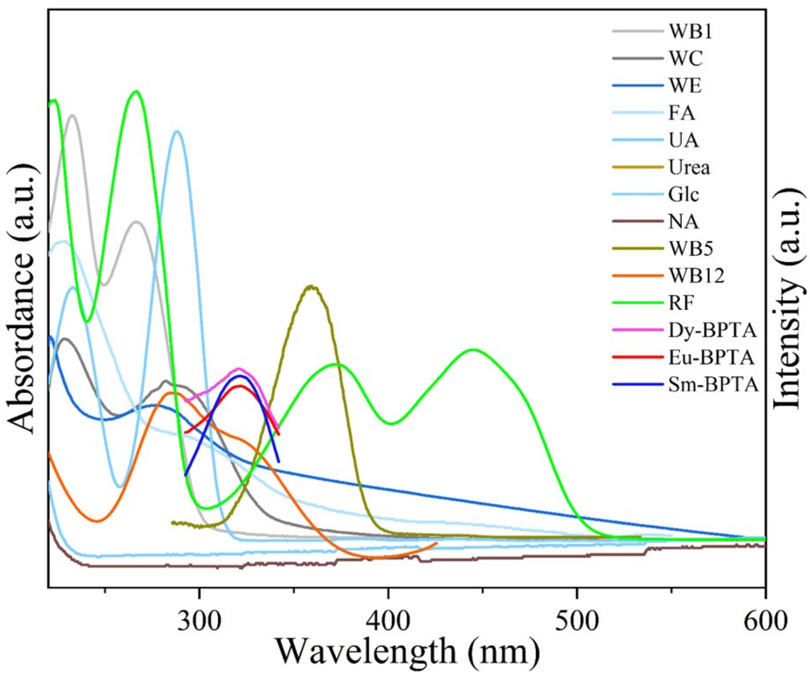

Fig. S28. UV absorption spectra of the interferents, excitation spectra of Ln-BPTA 1-3 and UV absorption spectrum of RF

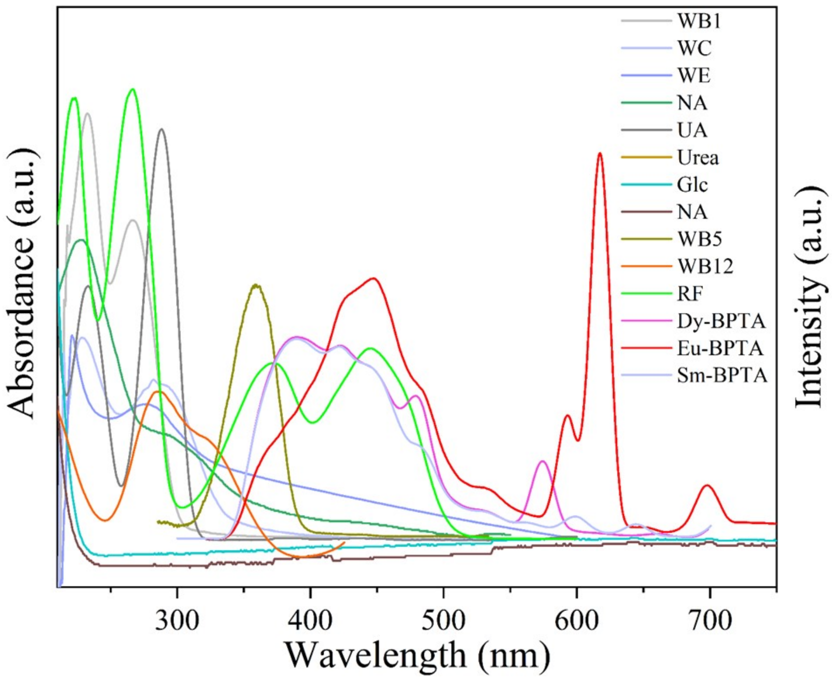

Fig. S29 UV absorption spectra of the interferents, emission spectra of Ln-BPTA 1-3 and UV absorption spectrum of RF.